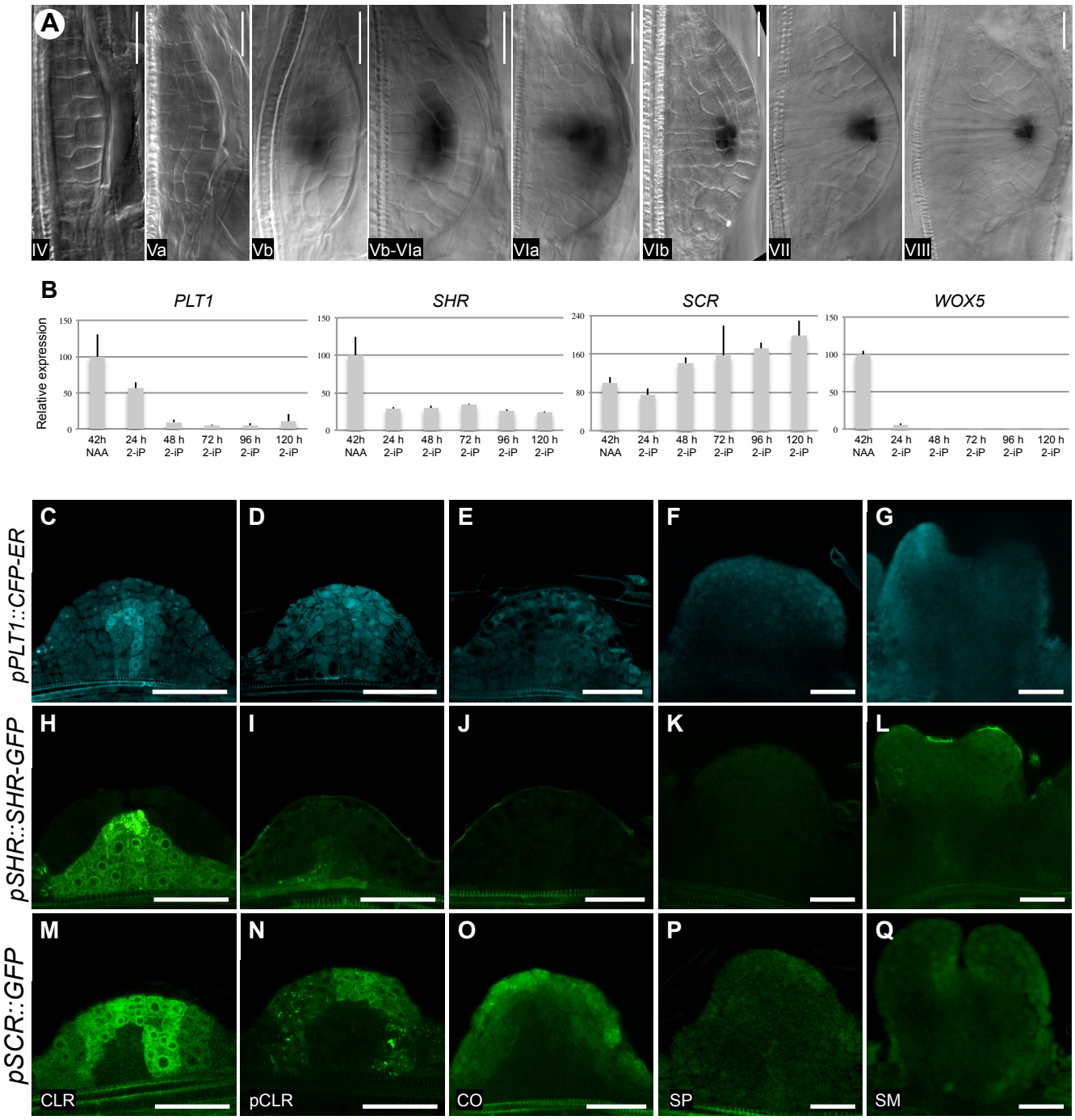

Figure S1: Expression of root identity genes during conversion.
A, Whole mount *in situ* localization of the *WOX5* transcript during lateral root development. Developmental stages indicated in the lower left corner of each picture are defined by Malamy and Benfey (1997). Lateral root were visualized with Nomarski microscopy (DIC). Scale bars: 20 µm. B, RT-qPCR analysis of *PLT1*, *SHR, SCR* and *WOX5* expression across the conversion in Col-0 explants. C, H and M: competent lateral root (CLR). *pPLT1::CFP-ER* marked CLR provascular domain, SHR protein was observed in the stele, and *SCR* was transcribed in the cell layers prefiguring the root cap, endodermis, pericycle, cortex and QC. D, I and N: paused competent lateral root primordium (pCLR). *PLT1* and *SCR* were transcribed at this stage, but *SHR* expression was rapidly turned off. E, J and O: converting organ (CO). Only transcription of *SCR* was observed. F, K and P: shoot promeristem (SP). Only transcription of *SCR* was observed. G, L and Q: shoot meristem (SM). The expression of *SCR* in the SAM can be detected. Conversion stages are as defined in Figure 2R. Reporter lines are indicated to the left of panels A to O. Scale bars: 50 µm.

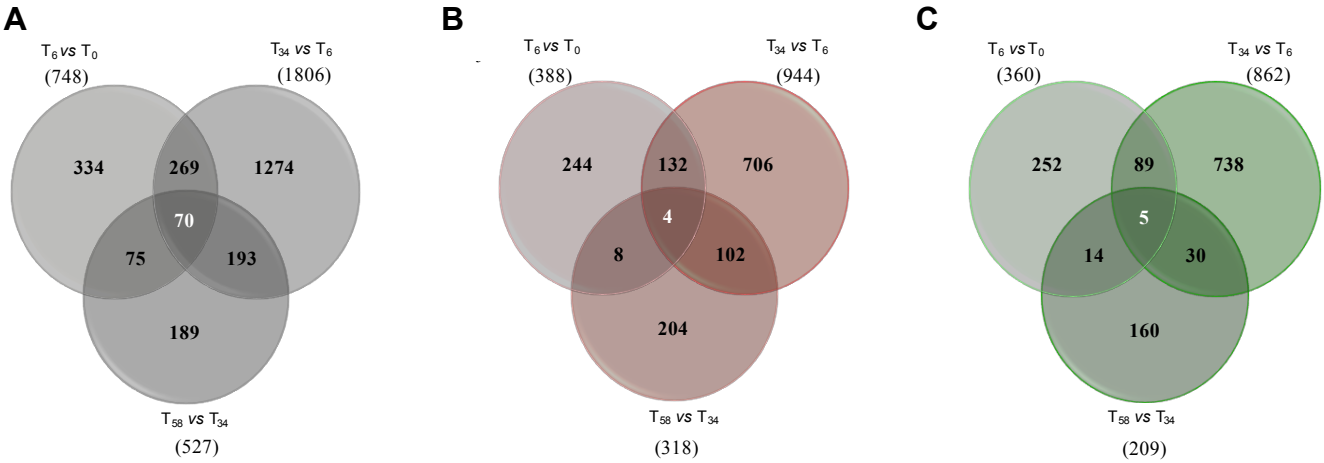

D

Comparisons	T6 vs T0		T34 vs T6		T58 vs T34	
DEG	All	Specific	All	Specific	All	Specific
Up-regulated	388	244	944	706	318	204
Down-regulated	360	252	862	738	209	160
Total	**748**	**334**	**1806**	**1274**	**527**	**189**

Figure S2: Distribution of differentially expressed genes.
A, Venn diagrams of the total; B, up-regulated and C, down-regulated genes DEGs identified in the T_6 *vs.* T_0, T_{34} *vs.* T_6, T_{58} *vs.* T_{34} comparisons. Numbers in parenthesis correspond to the total number of DEGs. Differentially expressed genes counted (Table S1) were selected by statistical analysis based on the Bonferroni method using a p-value cut-off of 0.05. D, Summary table.

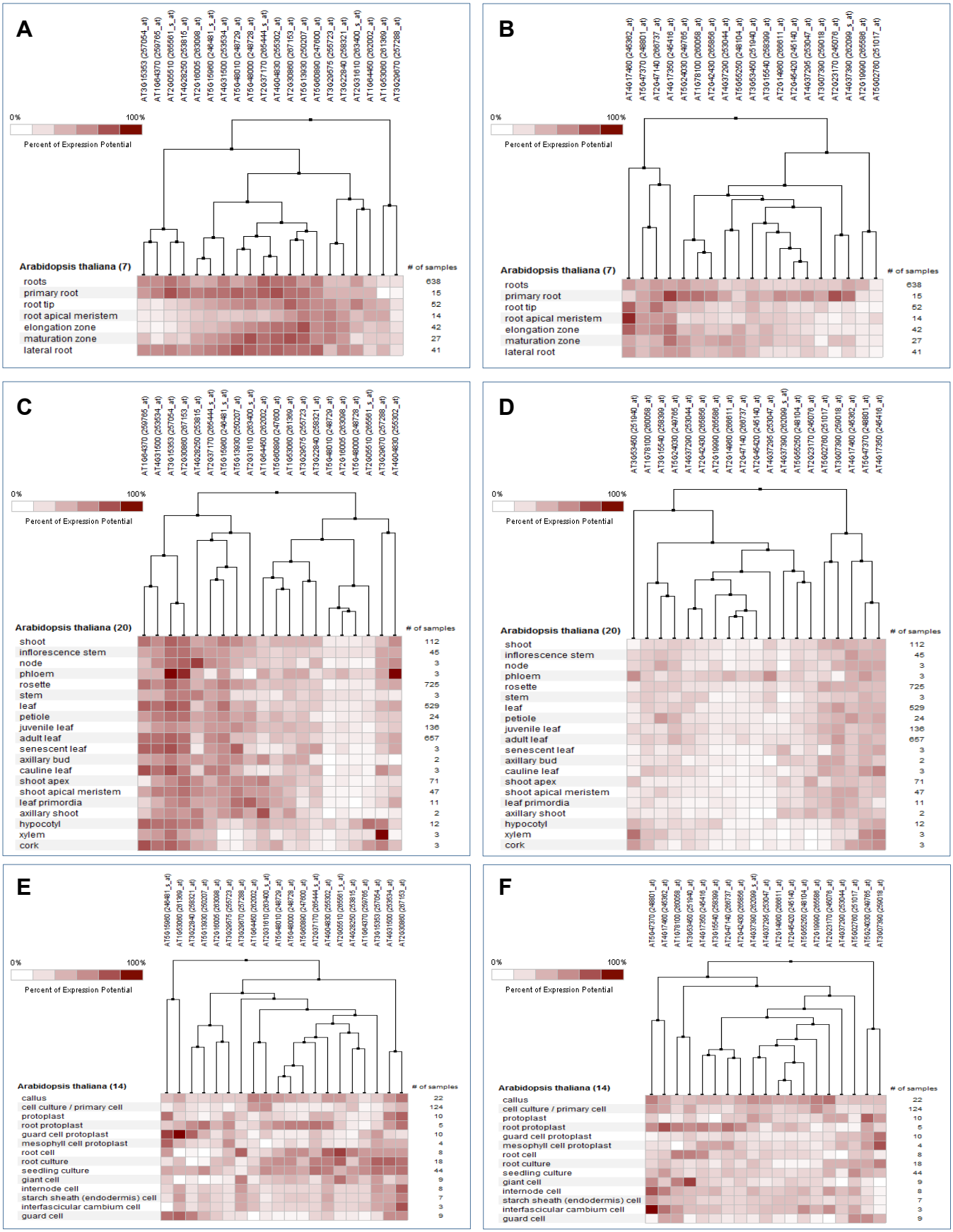

Figure S3: Comparison of our most DEGs with transcriptomic data sets.
Hierarchical clustering of the top 20 most up- (A, C, E, G, I, K, M, O, Q) or down-regulated (B, D, F, H, J, L, N, P, R) of T_6 *vs.* T_0 (A-F), T_{34} *vs.* T_6 (G-L) and T_{58} *vs.* T_{34} (M-R) comparisons with 7, 20 and 14 anatomical parts corresponding to root (A, B, G, H, M, N) shoot (C, D, I, J, O, P) and cell culture/primary cell (E, F, K, L, Q, R) transcriptomic data sets, respectively. A, Up-related DEGs from the T_6 *vs.* T_0 comparison correspond mostly to genes induced in 7 anatomical parts of the root and C, partially to genes induced in 20 anatomical parts of the shoot selection. I and J *vs.* O and P, The amount of genes induced in these later shoot selection increases in T_{34} *vs.* T_6 comparison gene set to become the main anatomical selection in which most of the genes up-regulated set from the T_{58} *vs.* T_{34} comparison are regulated.

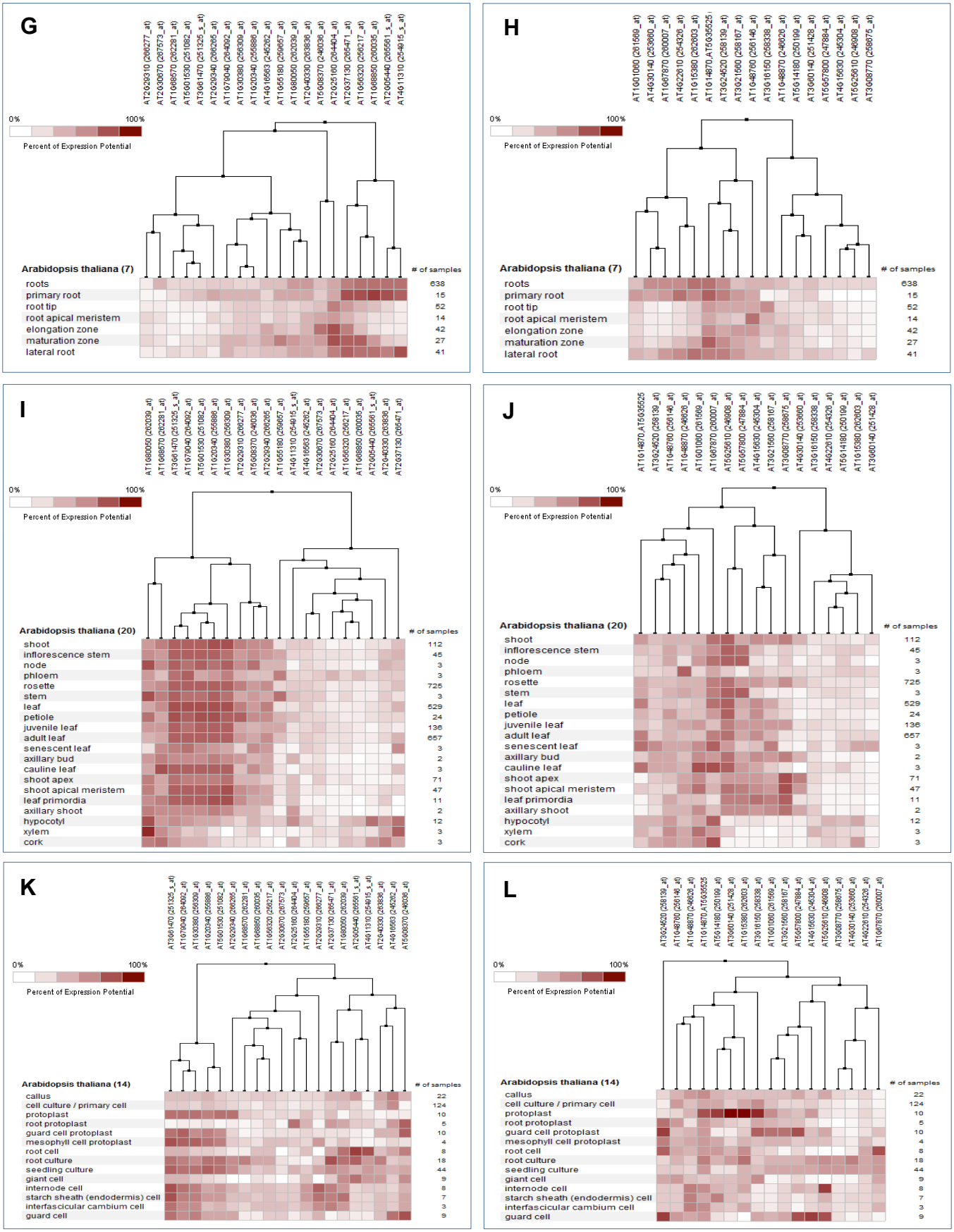

Figure S3: Comparison of our most DEGs with transcriptomic data sets.
Hierarchical clustering of the top 20 most up- (A, C, E, G, I, K, M, O, Q) or down-regulated (B, D, F, H, J, L, N, P, R) of T_6 *vs.* T_0 (A-F), T_{34} *vs.* T_6 (G-L) and T_{58} *vs.* T_{34} (M-R) comparisons with 7, 20 and 14 anatomical parts corresponding to root (A, B, G, H, M, N) shoot (C, D, I, J, O, P) and cell culture/primary cell (E, F, K, L, Q, R) transcriptomic data sets, respectively. A, Up-related DEGs from the T_6 *vs.* T_0 comparison correspond mostly to genes induced in 7 anatomical parts of the root and C, partially to genes induced in 20 anatomical parts of the shoot selection. I and J *vs.* O and P, The amount of genes induced in these later shoot selection increases in T_{34} *vs.* T_6 comparison gene set to become the main anatomical selection in which most of the genes up-regulated set from the T_{58} *vs.* T_{34} comparison are regulated.

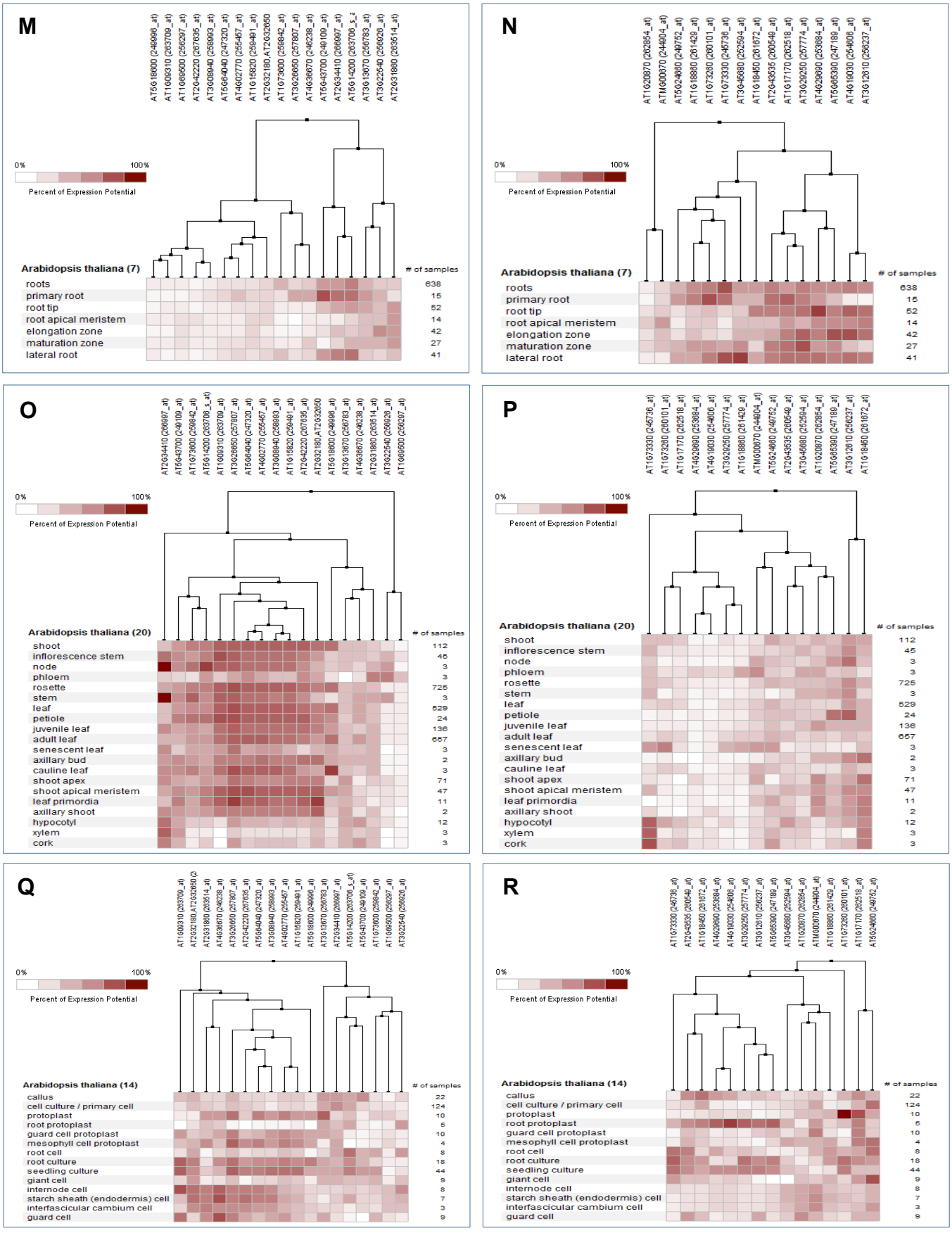

Figure S3: Comparison of our most DEGs with transcriptomic data sets.
Hierarchical clustering of the top 20 most up- (A, C, E, G, I, K, M, O, Q) or down-regulated (B, D, F, H, J, L, N, P, R) of T_6 *vs.* T_0 (A-F), T_{34} *vs.* T_6 (G-L) and T_{58} *vs.* T_{34} (M-R) comparisons with 7, 20 and 14 anatomical parts corresponding to root (A, B, G, H, M, N) shoot (C, D, I, J, O, P) and cell culture/primary cell (E, F, K, L, Q, R) transcriptomic data sets, respectively. A, Up-related DEGs from the T_6 *vs.* T_0 comparison correspond mostly to genes induced in 7 anatomical parts of the root and C, partially to genes induced in 20 anatomical parts of the shoot selection. I and J *vs.* O and P, The amount of genes induced in these later shoot selection increases in T_{34} *vs.* T_6 comparison gene set to become the main anatomical selection in which most of the genes up-regulated set from the T_{58} *vs.* T_{34} comparison are regulated.

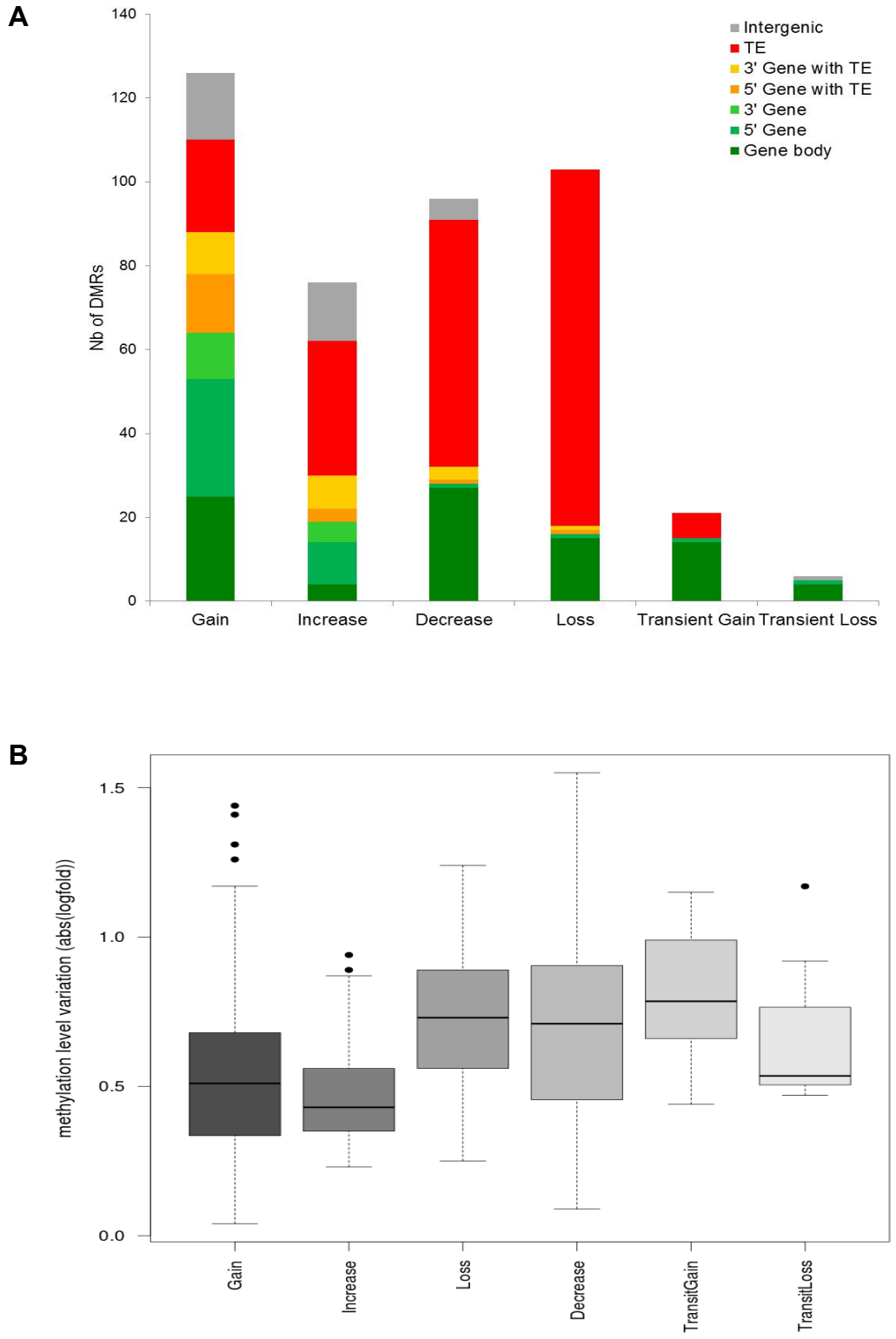

Figure S4: A limited number of low amplitude DMRs are detected across the conversion sequence.

A, Distribution of DMRs according to patterns of DNA methylation variation. Gain, continuous methylation increase, from unmethylated state at T_0 to higher methylation level at T_{58}. Loss, continuous methylation decrease, down to unmethylated at T_{58}. Increase and Decrease, positive and negative changes between intermediate methylation levels during conversion, respectively. Transient Gain and Transient Loss, higher and lower level of methylation in T_6 and T_{34} in comparison to T_0 and T_{58}, respectively. B, Average fold-change in DNA methylation levels according to patterns of DNA methylation variation.

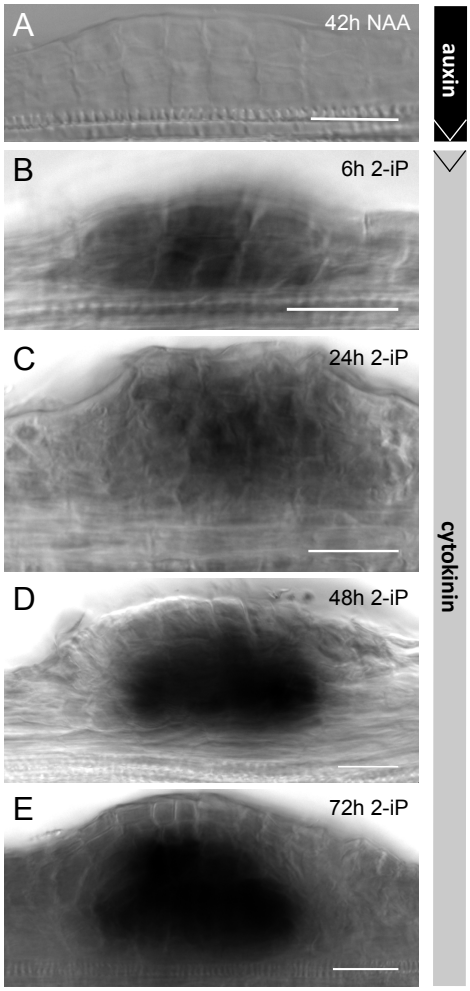

Figure S5: Expression of *WUS* in lateral root primordia induced with exogenous cytokinin at stage V.
Whole mount root segments were hybridized *in situ* with the *WUS* antisense probe after auxin (NAA) priming (A), and subsequent cytokinin (2iP) induction (B-E). Lateral organs were visualized with Nomarski microscopy (DIC). Scale bars: 20 µm.

Table S1: Differentially expressed genes (DEGs) between consecutive time points in the conversion sequence (cf : Table S1.xls)

Click here to Download Table S1

Table S2: Comparisons with published microarray data. Synthesis of the number of genes in commun between our study and query lists of genes involved in metabolism and dowstream signaling of auxin and cytokinin (Nemhauser et al., 2006; Brenner and Schmülling, 2015), in cell cycle (Vandepoele et al., 2002; Chatfield et al., 2013), in regeneration of shoots, calli or roots in tissue culture from Arabidopsis (Che et al., 2006) and in regeneration of shoots obtained in tissue culture from Arabidopsis mutant affected in DNA methylation (Li et al., 2011 ; see Supplemental Experimental Procedures for details). Percents in black correspond to set of genes found in commun studies or query lists significantly enriched at the significant threshold of hypergeometric and Bonferonni test p-value<0.05. preCIM : preculture on Callus-Inducing Medium, SIM : Shoot-Inducing Medium, CIM : Callus-Inducing Medium, RIM : Root-Inducing Medium. *: DEG that have been subtracted from EUGENE predictions and genes encoding microRNAs or predicted to encode HypmiRNAs.

DEGs in this study*			*T6 (vs T0)*			*T34 (vs T6)*			*T58 (vs T34)*		
			up	down	Total	up	down	Total	up	down	Total
			378	359	738	935	849	1784	305	200	505
Brenner and Schmülling (2015)	Cytokinin	up	6%	0%	3%	2%	0%	1%	1%	7%	3%
		down	0%	1%	0%	0%	0%	0%	0%	0%	0%
Nemhauser et al. (2006)			9%	4%	7%	6%	5%	5%	4%	11%	7%
Nemhauser et al. (2006)	Auxin		12%	21%	17%	8%	6%	7%	9%	13%	10%
Vandepoele et al. (2002) Chatfield et al. (2013)	Cell cycle		1%	3%	2%	0%	1%	1%	1%	0%	0%
Che et al. (2006)	preCIM	up	23%	43%	33%	12%	32%	21%	5%	8%	6%
		down	29%	17%	23%	24%	6%	15%	4%	10%	6%
	SIM		10%	1%	5%	1%	0%	0%	10%	6%	8%
	CIM		1%	2%	1%	1%	1%	1%	1%	1%	1%
	RIM		5%	3%	4%	7%	2%	4%	4%	3%	4%
Li et al. (2011)	M0/S0		7%	7%	7%	11%	3%	7%	21%	3%	14%
	M0 in S6/S0		3%	1%	2%	8%	1%	5%	17%	2%	11%

Table S3: Biological pathways significantly over-represented among deregulated genes. Significant pathways are in bold. ns: not significant.

	MAPMAN Classification	Frequency	T_6 *vs.* T_0 ± *bootstrap StdDev*	p-value	Frequency	T_{34} *vs.* T_6 ± *bootstrap StdDev*	p-value	Frequency	T_{58} *vs.* T_{34} ± *bootstrap StdDev*	p-value
Up –regulated genes	amino acid metabolism	**3.02**	***0.949***	**2.328e-03**	**3.17**	***0.629***	**9.105e-07**	ns	ns	ns
	cell	ns	ns	ns	**0.56**	***0.156***	**7.173e-03**	ns	ns	ns
	cell wall	ns	ns	ns	**2.42**	***0.367***	**5.380e-07**	ns	ns	ns
	development	**1.88**	***0.458***	**5.288e-03**	**1.5**	***0.249***	**5.530e-03**	ns	ns	ns
	DNA	**0.19**	***0.065***	**1.293e-09**	**0.11**	***0.035***	**1.489e-27**	**0.2**	***0.085***	**7.267e-08**
	gluconeogenesis / glyoxylate cycle	ns	ns	ns	**8.29**	***4.266***	**4.636e-03**	ns	ns	ns
	glycolysis	**3.23**	***0.744***	**3.813e-06**	ns	ns	ns	ns	ns	ns
	hormone metabolism	ns	ns	ns	**2.32**	***0.457***	**2.658e-06**	ns	ns	ns
	metal handling	ns	ns	ns	**3.46**	***1.304***	**1.684e-03**	ns	ns	ns
	micro RNA, natural antisense etc	ns	ns	ns	**0.07**	***0.057***	**2.809e-05**	ns	ns	ns
	minor CHO metabolism	ns	ns	ns	**3.76**	***1.05***	**3.434e-05**	ns	ns	ns
	miscaellous	**2.42**	***0.327***	**4.149e-08**	**2.39**	***0.191***	**4.854e-17**	**1.75**	***0.339***	**2.022e-03**
	N-metabolism	**10.09**	***5.15***	**2.962e-03**	**6.91**	***2.858***	**6.022e-04**	ns	ns	ns
	not assigned	**0.67**	***0.057***	**3.438e-07**	**0.65**	***0.035***	**2.227e-16**	**0.72**	***0.077***	**6.575e-05**
	nucleotide metabolism	**3.4**	***1.127***	**3.675e-03**	ns	ns	ns	ns	ns	ns
	protein	**0.37**	***0.081***	**1.191e-08**	**0.54**	***0.056***	**2.637e-10**	ns	ns	ns
	photosynthesis	ns	ns	ns	**5.58**	***0.986***	**2.818e-15**	**17.71**	***2.792***	**2.987e-32**
	redox	ns	ns	ns	**2.39**	***0.641***	**1.533e-03**	ns	ns	ns
	S-assimilation	**26.92**	***13.842***	**1.084e-05**	ns	ns	ns	ns	ns	ns
	secondary metabolism	**4.92**	***0.855***	**6.805e-11**	**3.39**	***0.538***	**5.097e-12**	**2.41**	***0.794***	**6.026e-03**
	signalling	**0.44**	***0.188***	**6.760e-03**	ns	ns	ns	ns	ns	ns
	stress	**1.78**	***0.33***	**2.085e-03**	**1.43**	***0.203***	**2.819e-03**	ns	ns	ns
	tetrapyrrole synthesis	ns	ns	ns	**5.24**	***2.003***	**2.948e-04**	17.89	*5.554*	**1.358e-08**
	transport	**2.48**	***0.438***	**5.095e-06**	**1.93**	***0.253***	**1.556e-06**	ns	ns	ns
Down-regulated genes	DNA	**0,5**	***0,13***	**4,26E-04**	**0,22**	***0,047***	**3,22E-18**	**0,1**	***0,055***	**3,05E-07**
	fermentation	ns	ns	ns	ns	ns	ns	**22,96**	***14,315***	**3,25E-03**
	hormone metabolism	**3,78**	***0,83***	**9,80E-08**	ns	ns	ns	**4,75**	***1,211***	**2,72E-07**
	lipid metabolism	**2,38**	***0,677***	**4,60E-03**	ns	ns	ns	ns	ns	ns
	miscaellous	**2,22**	***0,322***	**2,38E-06**	ns	ns	ns	**2,93**	***0,539***	**1,53E-07**
	not assigned	**0,68**	***0,067***	**1,60E-06**	**0,63**	***0,036***	**9,16E-17**	**0,59**	***0,081***	**3,32E-06**
	nucleotide metabolism	ns	ns	ns	**3,48**	***0,913***	**1,26E-05**	ns	ns	ns
	protein	**0,51**	***0,093***	**1,88E-05**	**2**	***0,106***	**4,97E-29**	ns	ns	ns
	RNA	**1,37**	***0,2***	**6,29E-03**	**1,48**	***0,127***	**5,22E-06**	ns	ns	ns

Table S4: Most differentially expressed genes during conversion (cf : Table S4.xls)

Click here to Download Table S4

Table S5: Loci with coinciding DNA methylation and transcript level changes. Variation in methylation and expression levels are represented for the few DMRs corresponding to a gene showing a change in expression during the conversion process. Relative levels of methylation at the different time points are represented by a heatmap, from low (green) to high (red) and variations in expression of the corresponding gene are represented by arrows.

Methylation						Expression				
Domain name	methylation change	T_0	T_6	T_{34}	T_{58}	$T_0 \rightarrow T_6$	$T_6 \rightarrow T_{34}$	$T_{34} \rightarrow T_{58}$	Annotation	
Chr3:19229787..19230313	gain	0,40	0,47	0,78	1,53	↗	↗	→	AT3G51820	ATG4/CHLG/G4 (CHLOROPHYLL SYNTHASE)
Chr2:7926498..7927189	gain	0,16	0,56	0,48	1,24	↘	↗	→	AT2G18193	AAA-type ATPase family protein
Chr1:28900772..28901152	gain	-0,38	-0,28	0,20	0,46	↘	↗	↗	AT1G76930	ATEXT4 (EXTENSIN 4)
Chr3:17030490..17031209	gain	0,01	0,25	0,06	0,83	↘	→	→	AT3G46320	histone H4
Chr3:20638713..20639257	gain	-0,13	-0,27	0,14	0,53	→	→	↘	AT3G55610	P5CS2 (DELTA 1-PYRROLINE-5-CARBOXYLATE SYNTHASE 2)
Chr2:11552315..11552703	gain	-0,11	-0,22	0,32	0,44	↘	→	→	AT2G27050	EIL1 (ETHYLENE-INSENSITIVE3-LIKE 1)
Chr2:14393613..14393996	increase	1,09	1,58	1,78	1,93	↗	→	→	AT2G34060	peroxidase, putative
Chr4:17684540..17685089	decrease	1,85	1,63	1,76	1,22	↘	→	→	AT4G37640	ACA2 (CALCIUM ATPASE 2)
Chr1:12566595..12567299	loss	0,40	0,21	0,28	-0,21	↗	→	→	AT1G34400	unknown protein
Chr3:17483630..17484009	loss	0,79	0,40	0,80	0,24	↘	→	→	AT3G47420	glycerol-3-phosphate transporter, putative

Supplemental Experimental Procedures

Arabidopsis growth medium composition

Arabidopsis solid growth medium consisted of MS salts with vitamins (Duchefa, M0222), supplemented with 0.5 $g.L^{-1}$ 2-(N-morpholino) ethane sulfonic acid (pH5.7; Sigma, M8250), 1 % (w/v) sucrose (Sigma, S9378). The gelling agent was 0.6 % (w/v) Agarose (Euromedex, D5) for Col-0 and 0.7% (w/v) Plant Agar (Duchefa, P1001) for L*er*. In explants sampled for RT-qPCR, transcriptomic and methylome studies, LR initiation was further synchronized by germinating and growing plantlets in the presence of the auxin transport inhibitor 1-N-naphthylphthalamic acid (NPA) prior to NAA priming. NPA first prevents the formation of auxin maxima and thus inhibits LR initiation. NAA then massively induces LR initiation along the primary root (Himanen et al., 2002). For these experiments, Col-0 plantlets were germinated and grown in the presence of 1.25 µM 1-N-Naphthylphthalamic acid (NPA) (Duchefa, N0926) for 6 d prior to NAA treatment. To induce lateral root formation, plantlets were transferred and grown for 42 hours on an auxin medium, similar to the previous one, but without NPA, and with 3.3 µM and 10 µM 1-naphthaleneacetic acid (NAA) (Duchefa, N0903) for Col-0 and L*er*, respectively. To induce shoot meristem formation, primary root segments were excised and transferred on a cytokinin medium, similar to the previous one but where auxin was replaced with 8.16 µM and 24.6 µM N6-[2-isopentenyl]adenine (2-iP) (Duchefa, D0906) for Col-0 and L*er*, respectively, and sucrose was replaced with 2% D-(+)-Glucose (Sigma, G8270) for all genotypes. The Col-0 x L*er* hybrid line was always treated as L*er*. In explants prepared for morphological and marker line analysis, LR initiation was induced with NAA priming for 42 h, but without NPA treatment during germination and growth on the first medium. Contrarily to the NPA treatment, this unsynchronized protocol avoids LRP fusion and was chosen as more convenient to follow the development of individual LRPs.

Phytohormones were dissolved in dimethylsulfoxide (DMSO; Sigma, D8418). Sugars and hormones were added to the media after autoclaving.

Arabidopsis reporter lines	Background	Reference
pWUS::GUS	Col-0xL*er*	(Gross-Hardt et al., 2002)
pPLT1::CFP	Col-0	(Aida et al., 2004)
pSHR::SHR-GFP	Col-0	(Helariutta et al., 2000)
pSCR::mGFP5-ER	Col-0	(Wysocka-Diller et al., 2000)
pCLV3::CFP-ER	L*er*	(Tucker et al., 2008)
pKNOLLE::KNOLLE-GFP	L*er*	(Boutté et al., 2010)
pPIN1:PIN1-GFP	L*er*	(Vernoux et al., 2000)
pCYCB1;1::DB-GUS	Col-0	(Colón-Carmona et al., 1999)
pTCSn ::GFP	Col-0	Gift from B. Müller
pPIN1::PIN1 :GFP/pSTM::STM :YFP	L*er*	NASC N66314
pDR5::rev:3XVENUS-N7/pCUC2::RFP	Col-0	Gift from P. Laufs
p35S::DII-VENUS	Col-0	(Brunoud et al., 2012)

Quantification of the conversion and reversion *in vitro* responses

Conversion. The distribution of converted organs was assessed relative to the LRP stages of development (Malamy and Benfey, 1997) at the onset of cytokinin treatment. A total of 210 Col-0 roots segments were analyzed carrying 4453 LRPs classified in three classes when transferred on 2-iP medium: stages V and younger ($n_{LRP\leq V}$ = 432, 7 converted in SMs, 0.7% of converted LRPs); stages VI and VII ($n_{LRP\ VIorVII}$ = 1716, 967 SMs; 90.2%); stages VIII and emerged ($n_{LRP\geq VIII}$ = 2305, 98 SMs; 9.1%). Conversion was assessed for each individual LR after 6 days of 2-iP treatment, by comparing images acquired at the beginning and at the end of the treatment.

Rates measured in a separate experiment showed that Landsberg *erecta* (L*er*) LRPs have a similar ability to convert according to their developmental stages: $n_{LRP\leq V}$ = 55, 6 SMs, 3.0%; $n_{LRP\ VIorVII}$ = 485, 175 SMs, 89.3%; $n_{LRP\geq VIII}$ = 162, 15 SMs, 7.7%. The conversion from an LR into an established SM is slower in L*er* than in Col-0, five days instead of four in our hands, which may be explained by the different gelling agent and hormone concentrations that were optimized empirically for both ecotypes.

For clarity, the lateral organs were preferentially labeled according to their developmental time, determined based to their structure, rather that their incubation time on 2-iP medium that varied slightly between ecotypes and transgenic markers lines.

Reversion. The distribution of reverted LRPs was assessed in excised root segments primed with NAA for 42h. A total of 73 Col-0 root segments carrying 8546 lateral roots at different stages were transferred on 2-iP medium for 3 d, then split in two batches: 3986 LRs (33 root segments) remained on the 2-iP medium for 3 more days, of which 1286 switched into shoot meristem development (conversion); 4560 LRs (40 root segments) were transferred back on NAA medium for 3 d, of which only 139 shoot promeristems did not switch back into LRPs (reversion).

Propidium iodide staining, confocal microscopy and image analysis

The protocol was adapted from (Truernit et al., 2008). Explants were fixed and stained with propidium iodide. The developing lateral organs were imaged as stacks of confocal optical sections and their organization was analyzed in the sagittal plane reconstructed for each object. Briefly, the explants were fixed in a 75% ethanol / 25% acetic anhydride solution for 2 d. Samples were rehydrated by successive immersion in 50%, 30% and 10% ethanol, and washed 3 times in distilled water. Amyloplasts were dissolved with amylase (0.2 mg/ml) for 3 h at 37 °C. Fixed explants were washed 3 times in distilled water, incubated in 1% periodic acid for 20 min, rinsed again with water, and stained overnight in Schiff reagent with propidium iodide (PI) (100 mM sodium metabisulphite, 0.15 N HCl, freshly added PI at a final concentration of 0.1 mg/µl). Samples on microscope slides were covered with a chloral hydrate solution (4 g chloral hydrate, 1 mL glycerol, 2 mL water) after 3 washes in water. Explants were imaged with a Leica SP5 spectral confocal laser scanning microscope (Leica Microsystems). Excitation wavelength for PI–stained samples was 488 nm, emission signal was collected from 520 to 720 nm. Acquired Z stacked images (lif format) were converted (tif format) with ImageJ (V1.46, 64 bits). See Table below for voxel size. Stacks were reoriented according to the main axis of the primary root to define the transverse and sagittal planes passing through the center of the LRP by 3D multi-planar reconstruction with the OsiriX software (V.5.6, 32 bits). LRP developmental stages were identified based on the number of epidermal cells and the organization of the cells in the stele, as observed in the reconstructed sagittal plane.

Voxel sizes in images of propidium iodide-stained explants

	Panel	Width	Height	Depth
Figure 2	E	0.2225987	0.2225987	0.4196171
	F	0.2225986	0.2225986	0.4196171
	G	0.1082093	0.1082093	0.293732
	H	0.158513	0.158513	0.2098085
	I	0.2225987	0.2225987	0.4196171
	J	0.2225987	0.2225987	0.7133491
	K	0.3029291	0.3029291	1.0070810
	L	0.2225987	0.2225987	0.7133491
	M	0.2225986	0.2225986	
Figure 3	A	0.1224285	0.1224285	0.293732
	B	0.1650829	0.1650829	0.7133491
	C	0.2225986	0.2225986	0.7133491
	D	0.2225986	0.2225986	0.7133491
	E	0.2225986	0.2225986	0.4196171
	F	0.4451973	0.4451973	0.7133491

GUS staining and quantification

Tissues were fixed in ice-cold 90% acetone for 10 min on ice, rinsed with water for 5 min, vacuum infiltrated for 5 min with staining solution (50 mM sodium phosphate buffer pH 7, 0.2% Triton-X-100, 2 mM potassium ferrocyanide, 2 mM potassium ferricyanide, 1 mM X-gluc) and incubated at 37°C for 7 to 18 h. The reaction was stopped with 70% ethanol and conserved at 4°C until observation. The samples were mounted in 10% glycerol and photographs were taken with a Zeiss Axio zoom stereo-microscope.

To quantify the cell division average in the converting organs, the number of blue GUS-stained spots were counted in *pCYCB1;1::DB-GUS* explants to measure the number of dividing cells in a converting organ and averaged per developmental stage: CLR at stage VI or VII (NAA 42 h, n=160); pCLR (2-iP 24 and 48 h, n=57 of which 24 showed no GUS spot); CO (2-iP 72 h, n=35); SP (2-iP 96 h,

n=40); SM (2-iP 120 h, n=14).

Quantitative real-time RT-PCR analysis

Total RNA was isolated with the RNeasy Plant mini-kit (Qiagen). For RT-qPCR, 5 µg of RNAs were DNase-treated using DNaseI according to the manufacturer's instructions (Qiagen) and cDNAs were synthesized using oligo(dT) with Superscript II reverse transcriptase (Invitrogen) according to the manufacturer's instructions. Quantitative real-time RT-qPCR was performed in an Eppendorf Mastercycler realplex (Eppendorf) with MESA GREEN qPCR MasterMix Plus for SYBRAssay (Eurogentec) as per manufacturer's instructions. Data analysis, including calculation of primer pair reaction efficiencies and Ct values, was carried out by Eppendorf Manager software. The results of two technical replicates of two biological samples were normalized with 1 to 4 genes with a steady level of transcription. The first point of the kinetic is used as the 100% reference for the normalization of the relative expression. All RT-qPCR data points were obtained with 60-80 pooled explants. Each explants harbored dozens of converting/reverting primordia at synchronized developmental stages. List of primers pairs used in RT-qPCR experiments:

Gene name	5' primer	3' primer
WUS	gtgttcccatgcagagacct	tcagtacctgagcttgcatga
STM	ccaagatcatggctcatcct	cctgttggtcccatagatgc
WOX5	ggagaggcagaaacgtcgta	tgaattcaccggaaagagttg
PLT1	gccggaaacaaagacctctac	aatggctttcacgtcgtacc
SHR	gagacagcgaggaagtggtc	ccatcgaccaaacaccttct
SCR	tgaggaaaagggaagctgtg	agcgtggctcaaatcttgtt
CLV3	gtccggtccagttcaacaac	gcttctccatttgctccaac
CUC2	aaggaagagctccgaaagga	tccggtgctagctaaagtgg
Ubq5	cttgaagacggccgtaccctc	cgctgaacctttcaagatccatcg
AT5G13440	acaagccaatttttgctgagc	acaacagtccgagtgtcatggt
AT2G26060	gggatggtcaagatttggca	caaaccaacagcagtcacggt
AT429130	ggcgttttctgatagcgaaaa	atggatcaggcattggagct
HIS4	cgaagattggctcgtagagg	gctcggtgtaagtgacagca
CYCB2;4	ggatacgaggattggagcaa	ttgtgatgcaaaccaaccat
KRP2	ggtgacgatcgtgaaacaga	aagatctttctccgccacct
RGF1	gtgaaggtcttggagcaagc	tctcatttgcctccaccttc
LBD16	ccatgatcgatgtgaagctg	ggttggtactttccgagctg
LBD18	aggtccgatgctgtcgtaac	gatgccaaatgggcttgtaa
ARF16	tcaaatacgcaggaaacgaa	cgctctcacttccttgttcc
TMO5	gggttcgatggtgagatcat	acttccgctagcaaagaagc
TMO7	atgtcgggaagaagatcacg	cttgtaacaccctcgctgct
PID	tgaaaatgcttgaccatcca	actagaacttcggcggcata
IAA17	ggtatcaatggacggagcac	cccagctattcaccaaatcc
IAA19	tggatggtgtgccttatttg	cgagcatccagtctccatct
IAA28	taaagttctggtcggggatg	aaggcgtgggaggtcttta

Transcript profiling

Microarray analyses were carried out with the CATMA array containing 24,576 gene-specific tags corresponding to 22,089 genes and 633 mitochondrial and chloroplastic genome segments from *Arabidopsis thaliana* (Crowe et al., 2003; Hilson et al., 2004). To maximize specificity, the lateral organs were laser micro-dissected and pooled for transcript profile analysis at four time points: T_0, 42 h NAA-priming, competent lateral root (CLR); T_6, 6 h 2-iP treatment, paused CLR; T_{34}, 34 h 2-iP, converting organ (CO) resuming active cell division; T_{58}, 58 h 2-iP, early shoot primordium (eSP) (Fig. 5G). Total RNA was extracted from samples corresponding to the four time points in two independent biological experiments, with the Qiagen RNAeasy plant minikit according the manufacturer's instructions. For T_6 vs. T_0, T_{34} vs. T_6 and T_{58} vs. T_{34} comparisons, two technical replicates in dye-swap were performed for each of the two biological repeats. The labeling of cRNA with Cy3-dUTP or Cy5-dUTP (Perkin-Elmer- NEN Life Science Products), the hybridization to the slides, and the scanning were performed as described in Lurin et al. (2004). Specific statistics were developed to analyze CATMA hybridizations. For each array, the raw data comprises the logarithm of median feature pixel intensity (in log base 2) at wavelengths 635 nm (red) and 532 nm (green). No background was subtracted. The normalization method used is described in Lurin et al. *(*2004). To determine differentially expressed genes, we performed a pair t-test on the log ratios averaged on the dye-swap.

A trimmed variance is calculated from spots which do not display extreme variance. The raw p-value are adjusted by the Bonferroni method, which controls the Family Wise Error Rate (FWER) (with a type I error equal to 5%). We also adjusted the raw p-values to control a FDR using Benjamini-Yetkutieli at level 1%. Nonetheless, in the CATMA analysis pipeline, FWER proved to be the best solution to balance the estimated number of false positives and false negatives (Ge et al., 2003). As described in Gagnot et al. (2008), when the Bonferroni P value was lower than 0.05, the gene was considered differentially expressed. Hereafter, a transcript profile change at a given time point refers to a pairwise comparison with the previous time point. Accordingly, 748 genes were differentially expressed (DEGs) at T_6, 1806 at T_{34} and 527 at T_{58} (Table S1, Fig. S2).

Profiles were confirmed by real time RT-qPCR analysis for sets of genes involved in root meristem initiation or maintenance, cell cycle, and auxin metabolism (*RGF1*: AT5G60810, LBD16: AT2G42430, *LBD18*: AT2G45420, *IAA17*: AT1G04250, *IAA19*: AT3G15540, *IAA28*: AT5G25890, *TMO5*: AT3G25710, *TMO7*: AT1G74500, *PID*: AT2G34650, *KRP2*: AT3G50630, *CYCB2.4*: AT1G76310, *ARF16*: AT4G30080). Each gene profile was classified according to the statistically differential change(s), up or down, measured between the successive time points. Lists of set of genes specifically regulated across the conversion sequence are available in Table S1.

Biological pathways enrichment

Analyzed DEG sets correspond to genes significantly up- or down-regulated between two consecutive time points (Table S1). Biological pathways significantly over-represented (p-value < 0,01; Table S3) were identified with the classification superviewer tool of the university of Toronto website (http://bar.utoronto.ca/ntools/cgi-bin/ntools_classification_superviewer.cgi) using MAPMAN classification as a source (Provart and Zhu, 2003).

Comparative analysis of experimental data sets

The differentially expressed genes (DEGs) identified in our study (Table S1) were classified according to auxin or cytokinin metabolism and downstream signaling (in comparison to data sets published in Nemhauser et al., 2006), induced or repressed by cytokinin treatment (in at least three of four data sources as described in Brenner and Schmülling, 2015), involved in cell cycle (Vandepoele et al., 2002; Chatfield et al., 2013), or whether independent studies highlighted the same genes (Che et al., 2006; Li et al., 2011). Note that transcriptome data sets were produced with different microarray platforms. In our comparative analyses, genes tracked with Affymetrix chips were grouped according to the MAPMAN pathway classification, based on the Ath_Affy1_TAIR10_August 2012 Arabidopsis genome annotation. The genes tracked with the CATMA microarray were defined according to the EuGène prediction (Sclep et al., 2007). Hypergeometric tests were realized to determine if DEGs identified in this study were significantly over-represented in gene sets found in others. The comparable gene pool is defined as the 20,693 genes represented on both the ATH1 Affymetrix chips and the CATMA arrays (Table S2). To control for false positive results, raw p-values were adjusted with the Bonferroni correction. H_0, meaning that the overlap between our DEG lists and other gene sets is a random event, was rejected for adjusted p-value < 5% (Tables S1 and S2). Genes identically and specifically regulated between two consecutive time points were classified with the Venny software tool (http://bioinfogp.cnb.csic.es/tools/venny/). The list of genes in the intersections can be extracted from Table S1.

We examined whether DEGs identified in this study may be regulated by MET1-dependent DNA methylation by crossing our data with the results of Li et al. (2011) (Table S2). Li and coworkers showed that 768 genes were differentially regulated when comparing *met1-1* mutant (M0) *vs.* wild-type calli (S0), following a 20-day-culture on CIM medium (M0/S0 in Table S2). Among these, 308 genes were also differentially expressed in wild-type explants cultivated for 20 days on CIM (S0) and those transferred for 6 more days on SIM (S6) (M0 in S6/S0 in Table S2), suggesting that they might be induced on SIM and be regulated by MET1-dependent DNA methylation. A significant number of DEGs mostly induced at T_{34} and T_{58} were found to be over-represented in the 308 candidate genes pointing to the putative involvement of MET1-dependent transcriptional regulation during the conversion process.

Clustering

Hierarchical clustering analyses were performed via the Genevestigator online web tools (https://www.genevestigator.com/gv/), with the 20-most DEGs identified in this transcriptome study (Table S4), measured as Euclidian distance, and based on *Anatomy* and *Perturbation* data selections.

The *Anatomy* selection corresponds to 829, 2,394 and 281 hybridization results including 7, 20 and 14 anatomical parts from root, shoot and callus/cell culture/primary cell (only for wild-type), respectively (Fig. S3). The *Perturbation* selection corresponds to all wild-type genetic background experiments (5,825 hybridization results) available in Genevestigator. The same conclusions were drawn when matching the 200-most DEGs with anatomical parts (extracted from Table S1), indicating that similarity is not skewed by the size of the DEG sets (data not shown).

***In situ* hybridization**

Whole-mount *in situ* hybridization was performed using a protocol described by H. Morin and A. Bendahmane (Institute of Plant Sciences Paris-Saclay, France). Labeled RNA probes were produced by *in vitro* transcription from a PCR amplified fragment of *STM* (700 bp), *WOX5* (527 bp) and *WUS* (1003 bp), using a DIG-RNA labeling kit (Roche, cat. no. 11175025910). For antisense probes (as), T7 promoter sequence was added to 3' primers. A *WOX5* sense probe (s) was produced as a negative control, in this case T7 promoter sequence was added to a 5' primer of *WOX5*. *STM* and *WUS* RNA probes are hydrolyzed into fragments with an average size of 400–500 nt before hybridization.

STM as, 5'-tgtaatacgactcactatagggctcaaagcatggtggaggagg-3'
WOX5 as, 5'-tgtaatacgactcactatagggcagatctaatggcggtggatg-3'
WUS as, 5'-tgtaatacgactcactatagggcctagttcagacgtagctcaaga-3'
WOX5 s, 5'-tgtaatacgactcactatagggcacggtggagcagttgaagat-3'

The colorimetric detection was performed with "BCIP/NBT Color Development Substrate" (Promega, cat. no. S3771). Images were taken through optical longitudinal section of explants visualized by Nomarski microscopy (DIC) with an Axio Imager 2 ZEISS microscope.

Supplemental References

Aida, M., Beis, D., Heidstra, R., Willemsen, V., Blilou, I., Galinha, C., Nussaume, L., Noh, Y.-S., Amasino, R. and Scheres, B. (2004). The *PLETHORA* genes mediate patterning of the Arabidopsis root stem cell niche. *Cell* **119**, 109–120.

Boutté, Y., Frescatada-Rosa, M., Men, S., Chow, C.-M., Ebine, K., Gustavsson, A., Johansson, L., Ueda, T., Moore, I., Jürgens, G., et al. (2010). Endocytosis restricts Arabidopsis KNOLLE syntaxin to the cell division plane during late cytokinesis. *EMBO J.* **29**, 546–558.

Brenner, W. G. and Schmülling, T. (2015). Summarizing and exploring data of a decade of cytokinin-related transcriptomics. *Front. Plant Sci.* **6**, 29.

Brunoud, G., Wells, D. M., Oliva, M., Larrieu, A., Mirabet, V., Burrow, A. H., Beeckman, T., Kepinski, S., Traas, J., Bennett, M. J., et al. (2012). A novel sensor to map auxin response and distribution at high spatio-temporal resolution. *Nature* **482**, 103–106.

Chatfield, S. P., Capron, R., Severino, A., Penttila, P.-A., Alfred, S., Nahal, H. and Provart, N. J. (2013). Incipient stem cell niche conversion in tissue culture: using a systems approach to probe early events in *WUSCHEL*-dependent conversion of lateral root primordia into shoot meristems. *Plant J.* **73**, 798–813.

Che, P., Lall, S., Nettleton, D. and Howell, S. H. (2006). Gene expression programs during shoot, root, and callus development in Arabidopsis tissue culture. *Plant Physiol.* **141**, 620–637.

Colón-Carmona, A., You, R., Haimovitch-Gal, T. and Doerner, P. (1999). Technical advance: spatio-temporal analysis of mitotic activity with a labile cyclin-GUS fusion protein. *Plant J.* **20**, 503–508.

Crowe, M.L., Serizet, C., Thareau, V., Aubourg, S., Rouzé, P., Beynon, J.L., Hilson, P., Weisbeek, P., Van Hummelen, P., Reymond, P., et al. (2003). CATMA - A complete Arabidopsis GST database. *Nucleic Acids Res.* **31**, 156–158

Gagnot, S., Tamby, J.P., Martin-Magniette, M.L., Bitton, F., Taconnat, L., Balzergue, S., Aubourg, S., Renou, J.P., Lecharny, A., Brunaud, V. (2008). CATdb: a public access to Arabidopsis transcriptome data from the URGV-CATMA platform. *Nucleic Acids Res.* **36**, D986–990.

Ge, Y., Dudoit, S., Speed, T.P. (2003). Resampling-based multiple testing for microarray data analysis. *TEST* **12**, 1–44.

Gross-Hardt, R., Lenhard, M. and Laux, T. (2002). WUSCHEL signaling functions in interregional communication during Arabidopsis ovule development. *Genes Dev.* **16**, 1129–1138.

Helariutta, Y., Fukaki, H., Wysocka-Diller, J., Nakajima, K., Jung, J., Sena, G., Hauser, M. T. and Benfey, P. N. (2000). The *SHORT-ROOT* gene controls radial patterning of the Arabidopsis root through radial signaling. *Cell* **101**, 555–567.

Hilson, P., Allemeersch, J., Altmann, T., Aubourg, S., Avon, A., Beynon, J., Bhalerao, R., Bitton, F., Caboche, M., Cannoot, B., et al. (2004). Versatile Gene-Specific Sequence Tags for *Arabidopsis* Functional Genomics: transcript profiling and reverse genetics applications. *Genome Res.* **14**, 2176–2189.

Himanen, K., Boucheron, E., Vanneste, S., de Almeida Engler, J., Inzé, D. and Beeckman, T. (2002). Auxin-mediated cell cycle activation during early lateral root initiation. *Plant Cell* **14**, 2339–2351.

Li, W., Liu, H., Cheng, Z. J., Su, Y. H., Han, H. N., Zhang, Y. and Zhang, X. S. (2011). DNA methylation and histone modifications regulate de novo shoot regeneration in Arabidopsis by modulating *WUSCHEL* expression and auxin signaling. *PLoS Genet.* **7**, e1002243.

Lurin, C., Andrés, C., Aubourg, S., Bellaoui, M., Bitton, F., Bruyère, C., Caboche, M., Debast, C., Gualberto, J., Hoffmann, B. et al. (2004). Genome-wide analysis of Arabidopsis pentatricopeptide repeat proteins reveals their essential role in organelle biogenesis. *Plant Cell* **16**, 2089–2103.

Malamy, J. E. and Benfey, P. N. (1997). Organization and cell differentiation in lateral roots of Arabidopsis thaliana. *Development* **124**, 33–44.

Nemhauser, J. L., Hong, F. and Chory, J. (2006). Different plant hormones regulate similar processes through largely nonoverlapping transcriptional responses. *Cell* **126**, 467–475.

Provart, N. J. and Zhu, T. (2003). A Browser-based Functional Classification SuperViewer for Arabidopsis Genomics. *Curr. Comput. Mol. Biol.* 271–272.

Sclep, G., Allemeersch, J., Liechti, R., De Meyer, B., Beynon, J., Bhalerao, R., Moreau, Y., Nietfeld, W., Renou, J. P., Reymond, P., Kuiper, M. T. and Hilson P. (2007) CATMA, a comprehensive genome-scale resource for silencing and transcript profiling of Arabidopsis genes. *BMC Bioinformatics* **8**, 400.

Truernit, E., Bauby, H., Dubreucq, B., Grandjean, O., Runions, J., Barthélémy, J. and Palauqui, J.-C. (2008). High-resolution whole-mount imaging of three-dimensional tissue organization and gene expression enables the study of Phloem development and structure in Arabidopsis. *Plant Cell* **20**, 1494–1503.

Tucker, M. R., Hinze, A., Tucker, E. J., Takada, S., Jürgens, G. and Laux, T. (2008). Vascular signalling mediated by ZWILLE potentiates WUSCHEL function during shoot meristem stem cell development in the Arabidopsis embryo. *Development* **135**, 2839–2843.

Vandepoele, K., Raes, J., De Veylder, L., Rouzé, P., Rombauts, S. and Inzé, D. (2002). Genome-wide analysis of core cell cycle genes in Arabidopsis. *Plant Cell* **14**, 903–916.

Vernoux, T., Kronenberger, J., Grandjean, O., Laufs, P. and Traas, J. (2000). PIN-FORMED 1 regulates cell fate at the periphery of the shoot apical meristem. *Development* **127**, 5157–5165.

Wysocka-Diller, J. W., Helariutta, Y., Fukaki, H., Malamy, J. E. and Benfey, P. N. (2000). Molecular analysis of SCARECROW function reveals a radial patterning mechanism common to root and shoot. *Development* **127**, 595–603.